

---

# Local Spectral Clustering of Density Upper Level Sets

---

Anonymous Author(s)

Affiliation

Address

email

## Abstract

1 Spectral clustering methods are a family of popular nonparametric clustering tools.  
2 Recent works have proposed and analyzed *local* spectral methods, which extract  
3 clusters using locally-biased random walks around a user-specified seed node.  
4 Several authors have shown that local methods, such as personalized PageRank  
5 (PPR), have worst-case guarantees for certain graph-based measures of cluster  
6 quality. In contrast to existing works, we analyze PPR in a traditional statistical  
7 learning setup, where we obtain samples from an unknown distribution, and aim  
8 to identify connected regions of high-density (density clusters). We introduce  
9 two natural criteria for cluster quality, and derive bounds for these criteria when  
10 evaluated on empirical analogues of density clusters. Moreover, we prove that PPR,  
11 run on a neighborhood graph, extracts sufficiently salient density clusters. Finally,  
12 we provide empirical support of our theory.

## 13 1 Introduction

14 Let  $X = \{x_1, \dots, x_n\}$  be a sample drawn i.i.d. from a distribution  $\mathbb{P}$  on  $\mathbb{R}^d$ , with density  $f$ , and  
15 consider the problem of clustering: splitting the data into groups which satisfy some notion of  
16 within-group similarity and between-group difference. We focus on spectral clustering methods, a  
17 family of powerful nonparametric clustering algorithms. Roughly speaking, a spectral technique first  
18 constructs a geometric graph  $G$ , where vertices are associated with samples, and edges correspond  
19 to proximities between samples. It then learns a feature embedding based on the Laplacian of  $G$ ,  
20 and applies a simple clustering technique (such as k-means clustering) in the embedded feature  
21 space.

To be more precise, let  $G = (V, E, w)$  denote a weighted, undirected graph constructed from the  
samples  $X$ , where  $V = \{1, \dots, n\}$ , and  $w_{uv} = K(x_u, x_v) \geq 0$  for  $u, v \in V$ , and a particular  
kernel function  $K$ . Here  $(u, v) \in E$  if and only if  $w_{uv} > 0$ . We denote by  $\mathbf{A} \in \mathbb{R}^{n \times n}$  the  
weighted adjacency matrix, which has entries  $A_{uv} = w_{uv}$ , and by  $\mathbf{D}$  the degree matrix, with  
 $\mathbf{D}_{uu} = \sum_{v \in V} A_{uv}$ . We also denote by  $\mathbf{W}, \mathbf{L}$  the (lazy) random walk transition probability matrix  
and normalized<sup>1</sup> Laplacian matrix, respectively, which are defined as

$$\mathbf{W} = \frac{\mathbf{I} + \mathbf{D}^{-1}\mathbf{A}}{2}, \quad \mathbf{L} = \mathbf{I} - \mathbf{W},$$

22 where  $\mathbf{I} \in \mathbb{R}^{n \times n}$  is the identity matrix. Classical global spectral methods take a eigendecomposition  
23  $\mathbf{L} = \mathbf{U}\Sigma\mathbf{U}^T$ , use some number of eigenvectors (columns in  $\mathbf{U}$ ) as a feature representation for the  
24 samples, and then run (say) k-means in this new feature space.

25 When applied to geometric graphs constructed from a large number of samples, global spectral  
26 clustering methods can be computationally cumbersome and insensitive to the local geometry of  
27 the underlying distribution [Leskovec et al., 2010, Mahoney et al., 2012]. This has led to recent

---

<sup>1</sup>Other popular choices here include the unnormalized Laplacian, and symmetric normalized Laplacian.

increased interest in local spectral algorithms, which leverage locally-biased spectra computed using random walks around a user-specified seed node. A popular local clustering algorithm is Personalized PageRank (PPR), first introduced by [Haveliwala, 2003], and further developed by [Spielman and Teng, 2011, 2014, Andersen et al., 2006, Mahoney et al., 2012, Zhu et al., 2013], among others.

Local spectral clustering techniques have been practically very successful [Leskovec et al., 2010, Andersen et al., 2012, Gleich and Seshadhri, 2012, Mahoney et al., 2012, Wu et al., 2012], which has led many authors to develop supporting theory [Spielman and Teng, 2013, Andersen and Peres, 2009, Gharan and Trevisan, 2012, Zhu et al., 2013] that gives worst-case guarantees on traditional graph-theoretic notions of cluster quality (like conductance). In this paper, we adopt a more traditional statistical viewpoint, and examine what the output of a local clustering algorithm on  $X$  reveals about the unknown density  $f$ . In particular, we examine the ability of the PPR algorithm to recover *density clusters* of  $f$ , which are defined as the connected components of the upper level set  $\{x \in \mathbb{R}^d : f(x) \geq \lambda\}$  for some threshold  $\lambda > 0$  (a central object of central interest in the classical statistical literature on clustering, dating back to Hartigan [1981]).

## 1.1 Graph Connectivity Criteria

Here we define a pair of criteria that reflect the quality of a cluster with respect to  $G = (V, E, w)$ . There are many graph-based measures of cluster quality that one could consider; see, e.g., [Yang and Leskovec, 2015, Fortunato, 2010] for an overview. The pair of criteria that we focus on are (arguably) quite natural, and moreover, they play a fundamental role in our analysis of the PPR algorithm. Our two criteria capture the *external* and *internal* connectivity of a subset  $S \subseteq V$ , denoted  $\Phi(S; G)$  and  $\Psi(S; G)$ , respectively, and defined below in turn.

**External Connectivity: Normalized Cut** For subsets  $S, S' \subseteq V$ , we define the cut, degree, and volume functionals as usual,

$$\text{cut}(S, S'; G) = \sum_{u \in S} \sum_{v \in S'} w_{uv}, \quad \deg(u; G) = \sum_{v \in V} w_{uv}, \quad \text{vol}(S; G) = \sum_{u \in S} \deg(u; G).$$

As our notion of external connectivity, we use the *normalized cut* of  $S$ , defined as

$$\Phi(S; G) = \frac{\text{cut}(S; G)}{\min\{\text{vol}(S; G), \text{vol}(S^c; G)\}}, \quad (1)$$

where we abbreviate  $\text{cut}(S; G) = \text{cut}(S; S^c; G)$ .

**Internal Connectivity: Inverse Mixing Time** For  $S \subseteq V$ , denote by  $G[S] = (S, E_S, w_S)$  the subgraph induced by  $S$  (where the edges are  $E_S = E \cap (S \times S)$ ). Let  $\mathbf{A}_S, \mathbf{D}_S$  be the adjacency matrix and degree matrix, respectively, of  $G[S]$ . Define the (lazy) random walk matrix as usual,  $\mathbf{W} = \frac{\mathbf{D}_S^{-1} \mathbf{A}_S + \mathbf{I}_{|S| \times |S|}}{2}$ , and for  $v \in V$ , write

$$q_v^{(t)}(u) = e_v \mathbf{W}_S^t e_u$$

for the  $t$ -step transition probability of a random walk over  $G[S]$  originating at  $v$ .<sup>2</sup> Also write  $\pi = (\pi(u))_{u \in S}$  for the stationary distribution of this random walk. (Given the definition of  $\mathbf{W}_S$ , it is well-known that a unique stationary distribution exists and is given by  $\pi(u) = \deg(u; G[S]) / \text{vol}(S; G[S])$ .)

Our internal connectivity parameter will capture the time it takes for the random walk over  $G[S]$  to mix (approach the stationary distribution) uniformly over  $S$ . For this, we first define the *relative pointwise mixing time* of  $G[S]$  as

$$\tau_\infty(G[S]) = \min \left\{ t : \frac{\pi(u) - q_v^{(t)}(u)}{\pi(u)} \leq \frac{1}{4}, \text{ for } u, v \in V \right\}.$$

Now our internal connectivity parameter is simply the inverse mixing time,

$$\Psi(S; G) = \frac{1}{\tau_\infty(G[S])}. \quad (2)$$

<sup>2</sup>Given a starting node  $v$  and a random walk defined by transition probability matrix  $\mathbf{P}$ , the notation  $e_v \mathbf{P}^t$  is used to denote the distribution of the random walk after  $t$  steps.

56 If  $S$  has normalized cut no greater than  $\Phi$ , and inverse mixing time no less than  $\Psi$ , we call it as a  
 57  $(\Phi, \Psi)$ -cluster. Both local [Zhu et al., 2013] and global [Kannan et al., 2004] spectral algorithms  
 58 have been shown to output clusters (or partitions) which approximate the optimal  $(\Phi, \Psi)$ -cluster (or  
 59 partition) for a given graph  $G$ .<sup>3</sup>

## 60 1.2 PPR on a Neighborhood Graph

61 We now describe the clustering algorithm that will be our focus for the rest of the paper. We  
 62 start with the geometric graph that we form based on the samples  $X$ : for a radius  $r > 0$ , we  
 63 consider the  $r$ -neighborhood graph of  $X$ , denoted  $G_{n,r} = (V, E)$ , an unweighted graph with  
 64 vertices  $V = X$ , and an edge  $(x_i, x_j) \in E$  if and only if  $\|x_i - x_j\| \leq r$ , where  $\|\cdot\|$  denotes  
 65 Euclidean norm. Note that this is a special case of the general construction introduced above, with  
 66  $K(u, v) = 1(\|x_u - x_v\| \leq r)$ .

67 Next, we define the PPR vector  $p = p(v, \alpha; G_{n,r})$ , with respect to a seed node  $v \in V$  and a  
 68 teleportation parameter  $\alpha \in [0, 1]$ , to be the solution of the following linear system:

$$p = \alpha \mathbf{e}_v + (1 - \alpha)p\mathbf{W}, \quad (3)$$

69 where  $\mathbf{W}$  is the random walk matrix of the underlying graph  $G_{n,r}$  and  $\mathbf{e}_v$  denotes indicator vector  
 70 for node  $v$  (with a 1 in the  $v$ th position and 0 elsewhere). In practice, we can approximately solve the  
 71 above linear system via a simple, efficient random walk, with appropriate restarts to  $v$ .

72 For a level  $\beta > 0$  and a target volume  $\text{vol}_0 > 0$ , we define a  $\beta$ -sweep cut of  $p = (p_u)_{u \in V}$  as

$$S_\beta = \{u \in V : \frac{p_u}{\mathbf{D}_{uu}} > \frac{\beta}{\text{vol}_0}\}. \quad (4)$$

73 Having computed sweep cuts over a range  $\beta \in (\frac{1}{40}, \frac{1}{11})$ ,<sup>4</sup> we output a cluster  $\hat{C} = S_{\beta^*}$ , based on the  
 74 sweep cut  $S_{\beta^*}$  that minimizes the normalized cut  $\Phi(S_{\beta^*}; G_{n,r})$  as defined in (1). For concreteness,  
 75 we summarize this procedure in Algorithm 1.

---

### Algorithm 1 PPR on a Neighborhood Graph

---

**Input:** data  $X = \{x_1, \dots, x_n\}$ , radius  $r > 0$ , teleportation parameter  $\alpha \in [0, 1]$ , seed  $v \in X$ , target  
 stationary volume  $\text{vol}_0 > 0$ .

**Output:** cluster  $\hat{C} \subseteq V$ .

- 1: Form the neighborhood graph  $G_{n,r}$ .
- 2: Compute the PPR vector  $p(v, \alpha; G_{n,r})$  as in (3).
- 3: For  $\beta \in (\frac{1}{40}, \frac{1}{11})$  compute sweep cuts  $S_\beta$  as in (4).
- 4: Return  $\hat{C} = S_{\beta^*}$ , where

$$\beta^* = \arg \min_{\beta \in (\frac{1}{40}, \frac{1}{11})} \Phi(S_\beta; G_{n,r}).$$


---

## 76 1.3 Summary of Results

77 Let  $\mathbb{C}_f(\lambda)$  denote the connected components of the density upper level set  $\{x \in \mathbb{R}^d : f(x) > \lambda\}$ .  
 78 For a given density cluster  $\mathcal{C} \in \mathbb{C}_f(\lambda)$ , we call  $\mathcal{C}[X] = \mathcal{C} \cap X$  the *empirical density cluster*. Below  
 79 we give two notions of performance of a density cluster estimate.

80 **Definition 1** (Misclassification error). *For an estimator  $\hat{C} \subseteq X$  and set  $S \subseteq \mathbb{R}^d$ , the misclassification*  
 81 *error of  $S$  by  $\hat{C}$  is*

$$|\hat{C} \setminus (S \cap X)| + |(S \cap X) \setminus \hat{C}|. \quad (5)$$

---

<sup>3</sup>In the case of [Kannan et al., 2004], the internal connectivity parameter  $\phi$  is actually the conductance, i.e., the minimum normalized cut within the subgraph  $G[S]$ . See Theorem 3.1 in their paper for details; however, note that  $\phi^2 / \log(\text{vol}(S)) \leq O(\Psi)$ , and so the lower bound on  $\phi$  translates to a lower bound on  $\Psi$ .

<sup>4</sup>The choice of a specific range such as  $(\frac{1}{40}, \frac{1}{11})$  is standard in the analysis of PPR algorithms, see, e.g., [Zhu et al., 2013].

**Definition 2** (Consistent density cluster estimation). *For an estimator  $\hat{C} \subseteq X$  and cluster  $C \in \mathbb{C}_f(\lambda)$ , we say  $\hat{C}$  is a consistent estimator of  $C$  if for all  $C' \in \mathbb{C}_f(\lambda)$  with  $C \neq C'$  the following holds as  $n \rightarrow \infty$ :*

$$C[X] \subseteq \hat{C} \quad \text{and} \quad \hat{C} \cap C'[X] = \emptyset, \quad (6)$$

*with probability tending to 1.*

A summary of our main results (and outline for the rest of this paper) is as follows.

1. In Section 2, we derive in Theorem 1 an upper bound on the normalized cut of a (thickened) empirical density cluster  $C_\sigma[X]$ , under natural geometric conditions (precluding clusters that are arbitrarily thin).
2. Under additional geometric conditions, which exclude sets with large diameter or small bottleneck, we derive in Theorem 2 a lower bound on the inverse mixing time of a random walk over  $C_\sigma[X]$ .
3. In Section 3, we show in Theorems 3 and 4 that the bounds on the cluster quality criteria established in Theorems 1 and 2 have algorithmic consequences for PPR. Properly initialized, Algorithm 1 has low misclassification error with respect to a small enlargement of the set  $C$ , and if the density cluster  $C$  is particularly well-conditioned, Algorithm 1 will perform consistent density cluster estimation in the sense of (6). Corollary 1 establishes that these statements hold also with respect to an approximate form of PPR, which can be efficiently computed.
4. In Section 4, we empirically demonstrate the tightness of the bounds in Theorems 1 and 2, and provide examples showing how violations of the geometric conditions we require manifestly impact density cluster recovery by PPR.

On the topic of conditions, it is worth mentioning that, as density clusters are inherently local, focusing on the PPR algorithm actually eases our analysis and allows us to require fewer global regularity conditions relative to those needed for more classical global spectral algorithms.

## 1.4 Related Work

In addition to the background given above, a few related lines of work are worth highlighting. Global spectral clustering methods were first developed in the context of graph partitioning [Fiedler, 1973, Donath and Hoffman, 1973] and their performance is well-understood in this context (see, e.g., [Tolliver and Miller, 2006, von Luxburg, 2007]). In a similar vein, several recent works [McSherry, 2001, Rohe et al., 2011, Chaudhuri et al., 2012, Balakrishnan et al., 2011, Lei and Rinaldo, 2015, Abbe, 2018] have studied the efficacy of spectral methods in successfully recovering the community structure in the stochastic block model and variants.

Building on earlier work of [Koltchinskii and Gine, 2000], [von Luxburg et al., 2008, Hein et al., 2005] studied the limiting behaviour of spectral clustering algorithms. These authors show that when samples are obtained from a distribution, and we appropriately construct a geometric graph, the spectrum of the Laplacian converges to that of the Laplace-Beltrami operator on the data-manifold. However, relating the partition obtained using the Laplace-Beltrami operator to the more intuitively defined high-density clusters can be challenging in general.

Perhaps most similar to our results are the works [Vempala and Wang, 2004, Shi et al., 2009, Schiebinger et al., 2015], who study the consistency of spectral algorithms in recovering the latent labels in certain parametric and nonparametric mixture models. These results focus on global rather than local algorithms, and as such impose global rather than local conditions on the nature of the density. Moreover, they do not in general ensure recovery of density clusters, which is the focus in our work.

## 2 Cluster Quality Criteria Bounds for Density Clusters

### 2.1 Geometric Conditions on Density Clusters

In order to provide meaningful bounds on the normalized cut and inverse mixing time of an empirical density cluster, we must introduce conditions on the density  $f$ . Let  $B(x, r) = \{y \in \mathbb{R}^d : \|y - x\| \leq$

130  $r\}$  be the closed ball of radius  $r > 0$ , centered at  $x \in \mathbb{R}^d$ . Given a set  $\mathcal{A} \subseteq \mathbb{R}^d$  and  $\sigma > 0$ , define  
 131  $\mathcal{A}_\sigma = \mathcal{A} + B(0, \sigma) = \{y \in \mathbb{R}^d : \inf_{x \in \mathcal{A}} \|y - x\| \leq \sigma\}$ , which we call the  $\sigma$ -expansion of  $\mathcal{A}$ .  
 132 For a differentiable function  $g : \mathbb{R}^d \rightarrow \mathbb{R}^d$ , write  $\nabla g(x)$  to denote the Jacobian of  $g$  evaluated at  
 133  $x \in \mathbb{R}^d$ .

134 We are now ready to give our required conditions, stated with respect to a density cluster  $\mathcal{C} \in \mathbb{C}_f(\lambda)$   
 135 for some threshold  $\lambda > 0$ , and an expansion parameter  $\sigma > 0$ .

(A1) *Bounded density within cluster*: There are  $0 < \lambda_\sigma < \Lambda_\sigma < \infty$  such that

$$\lambda_\sigma = \inf_{x \in \mathcal{C}_\sigma} f(x) \leq \sup_{x \in \mathcal{C}_\sigma} f(x) \leq \Lambda_\sigma.$$

(A2) *Low noise density*: There exists  $\gamma, c_0 > 0$  such that for all  $x \in \mathbb{R}^d$  with  $0 < \text{dist}(x, \mathcal{C}_\sigma) \leq \sigma$ ,

$$\inf_{x' \in \mathcal{C}_\sigma} f(x') - f(x) \geq c_0 \text{dist}(x, \mathcal{C}_\sigma)^\gamma,$$

136 where  $\text{dist}(x, \mathcal{A}) = \inf_{x_0 \in \mathcal{A}} \|x - x_0\|$ .

(A3) *Cluster separation*: For all  $\mathcal{C}' \in \mathbb{C}_f(\lambda)$  with  $\mathcal{C}' \neq \mathcal{C}$ ,

$$\text{dist}(\mathcal{C}_\sigma, \mathcal{C}'_\sigma) > \sigma,$$

137 where  $\text{dist}(\mathcal{A}, \mathcal{A}') = \inf_{x \in \mathcal{A}} \text{dist}(x, \mathcal{A}')$ .

138 (A4) *Lipschitz embedding*: There exists  $\mathcal{K} \subseteq \mathbb{R}^d$  convex, and  $g : \mathbb{R}^d \rightarrow \mathbb{R}^d$  satisfying, for some  
 139  $L \geq 1$ ,

$$\det(\nabla g(x)) = 1, \frac{1}{L} \|x - y\| \leq \|g(x) - g(y)\| \leq L \|x - y\| \text{ for all } x, y \in \mathbb{R}^d$$

such that  $\mathcal{C}_\sigma$  is the image of  $\mathcal{K}$  by  $g$ ,  $\mathcal{C}_\sigma = g(\mathcal{K})$ . Furthermore, there exists  $D < \infty$  such  
 that for all  $x, x' \in \mathcal{K}$

$$\|x - x'\| \leq D.$$

140 Note that  $\sigma$  plays several roles here, precluding arbitrarily narrow clusters in (A1), flat densities  
 141 around the level set in (A2), and poorly separated clusters in (A3).

142 Assumptions (A1), (A2), and (A3) are used to upper bound  $\Phi(\mathcal{C}[X]; G_{n,r})$ , whereas (A1), and (A4)  
 143 are required to lower bound  $\Psi(\mathcal{C}[X]; G_{n,r})$ . We note that the lower bound on minimum density in  
 144 (A1) along with (A3) are similar to the  $(\sigma, \epsilon)$ -saliency of [Chaudhuri and Dasgupta, 2010], a standard  
 145 density clustering assumption, while (A2) is seen in, e.g., [Singh et al., 2009] (as well as many other  
 146 works on density clustering and level set estimation.) While (A4) may be less standard, as we will  
 147 see, it is critical in order to achieve reasonably tight bounds on  $\Psi(\mathcal{C}[X]; G_{n,r})$ . It is also worth  
 148 highlighting that these assumptions are all local in nature, a benefit of studying a local algorithm such  
 149 as PPR.

150 We emphasize that while many of these geometric conditions are typical in the density clustering  
 151 literature, the restrictions we will impose upon them in order to obtain meaningful implications for  
 152 PPR will not be. This is natural. The spectral algorithm we consider is not specifically designed for  
 153 the task of level set estimation, and in fact one should expect PPR to fail to recover – either in the  
 154 sense of (6), or indeed any reasonable notion of cluster recovery – a density cluster of sufficiently  
 155 large diameter or sufficiently small thickness (though we do not provide any lower bounds to this  
 156 effect). Indeed, one of the primary motivations of this work was to better understand and characterize  
 157 the distinctions between those level sets which are well conditioned for spectral algorithms, and those  
 158 which are not.

159 In the next several subsections, we will derive bounds on the cluster quality criteria evaluated on  
 160  $(\sigma$ -expansions of) density clusters. For notational simplicity, hereafter for  $S \subseteq V$ , we will abbreviate  
 161  $\Phi(S; G_{n,r})$  by  $\Phi_{n,r}(S)$ , and similarly,  $\Psi(S; G_{n,r})$  by  $\Psi_{n,r}(S)$ , and  $\tau_\infty(G_{n,r}[S])$  by  $\tau_{n,r}(S)$ . We  
 162 will also use  $\nu$  for Lebesgue measure on  $\mathbb{R}^d$ , and  $\nu_d = \nu(B)$  for the measure of the unit ball  
 163  $B = B(0, 1)$ .

## 2.2 Upper Bound on Normalized Cut

We start with an upper bound on the normalized cut (1) of  $\mathcal{C}_\sigma[X]$ . (In Theorem 1, the upper bound on the density in Assumption (A1) will not actually be needed, so we omit the parameter  $\Lambda_\sigma > 0$  from the theorem statement.) For  $\mathcal{S} \subseteq \mathbb{R}^d$  and  $r > 0$ , let

$$\pi_{\mathbb{P},r}(\mathcal{S}) := \frac{\int_{\mathcal{S}} \mathbb{P}(B(x,r))f(x)dx}{\int_{\mathbb{R}^d} \mathbb{P}(B(x,r))f(x)dx}.$$

**Theorem 1.** Fix  $\lambda > 0$ , and let  $\mathcal{C} \in \mathbb{C}_f(\lambda)$  satisfy Assumptions (A1), (A2), and (A3), for some  $\sigma, \lambda_\sigma, c_0, \gamma > 0$ . Let  $0 < r \leq \sigma/2d$  be such that

$$\pi_{\mathbb{P},r}(\mathcal{C}_\sigma) \leq \frac{1}{2}. \quad (7)$$

Then for any  $0 < \delta < 1$ ,  $\epsilon > 0$ , if

$$n \geq \frac{(2+\epsilon)^2 \log(3/\delta)}{\epsilon^2} \left( \frac{25}{6\lambda_\sigma^2 \nu(\mathcal{C}_\sigma) \nu_d r^d} \right)^2, \quad (8)$$

then

$$\frac{\Phi_{n,r}(\mathcal{C}_\sigma[X])}{r} \leq c_1 \frac{d}{\sigma} \frac{\lambda}{\lambda_\sigma} \frac{(\lambda_\sigma - c_0 \frac{r^\gamma}{\gamma+1})}{\lambda_\sigma} + \epsilon, \quad (9)$$

with probability at least  $1 - \delta$  (where  $c_1 > 0$  is a universal constant).

*Remark 1.* The proof of Theorem 1, along with all other proofs in this paper, can be found in the supplementary document. The key idea is that for any  $x \in \mathcal{C}$ , the simple fact  $B(x, \sigma) \subseteq \mathcal{C}_\sigma$  translates into the upper bound  $\nu(\mathcal{C}_\sigma + rB) \leq (1 + 2dr/\sigma)\nu(\mathcal{C}_\sigma)$ . We leverage (A2) to find a corresponding bound on the weighted volume, then apply standard concentration inequalities to convert from population- to sample-based results.

*Remark 2.* The inequality in (9) is tight in the case of  $\mathcal{C} = \{0\}$ . To see this, let  $\mathcal{C}_\sigma = B(0, \sigma)$  and

$$f(x) = \begin{cases} \lambda & \text{for } x \in \mathcal{C}_\sigma, \\ \lambda - \text{dist}(x, \mathcal{C}_\sigma)^\gamma & \text{for } 0 < \text{dist}(x, \mathcal{C}_\sigma) < r, \end{cases}$$

Then, some simple calculations yield

$$\mathbb{E}(\text{cut}(\mathcal{C}_\sigma[X]; G_{n,r})) \geq c\lambda\nu_d r^d \mathbb{P}((\mathcal{C}_\sigma + B(0, r))), \quad \text{and} \quad \mathbb{E}(\text{vol}_{n,r}(\mathcal{C}_\sigma[X]; G_{n,r})) \leq c'\lambda\nu_d r^d \mathbb{P}(\mathcal{C}_\sigma)$$

for some constants  $c, c' > 0$ . Thus the ratio  $\mathbb{E}(\text{cut}(\mathcal{C}_\sigma[X]; G_{n,r}))/\mathbb{E}(\text{vol}_{n,r}(\mathcal{C}_\sigma[X]; G_{n,r}))$  matches (9), up to constants.

## 2.3 Lower Bound on Inverse Mixing Time

Next we lower bound the inverse mixing time (2) of  $\mathcal{C}_\sigma[X]$ , or equivalently, as  $\Psi_{n,r}(\mathcal{C}_\sigma[X]) = 1/\tau_{n,r}(\mathcal{C}_\sigma[X])$ , we upper bound the mixing time.

**Theorem 2.** Fix  $\lambda > 0$ , and let  $\mathcal{C} \in \mathbb{C}_f(\lambda)$  satisfy Assumptions (A1) and (A4) for some  $\sigma, \lambda_\sigma, \Lambda_\sigma, D, K > 0$ . Then, for any  $0 < r < \sigma/2\sqrt{d}$ , with probability one

$$\limsup_{n \rightarrow \infty} \tau_{n,r}(\mathcal{C}_\sigma[X]) \leq c_2 \frac{\Lambda_\sigma^4 d^3 D^2 L^2}{\lambda_\sigma^4 r^2} \log^2 \left( \frac{1}{r} \right) + c_3 \log \left( \frac{\Lambda_\sigma}{\lambda_\sigma} \right) \quad (10)$$

for  $c_2, c_3 > 0$  universal constants.

Our proof technique involves two key geometric quantities: the *local spread*  $s(\tilde{G}_{n,r})$  (where we abbreviate  $\tilde{G}_{n,r} := G_{n,r}[\mathcal{C}_\sigma[X]]$  and let  $\tilde{\pi}_{n,r}$  be the stationary distribution over  $\tilde{G}_{n,r}$ ) and the *conductance*  $\tilde{\Phi}_{n,r}$ , defined respectively as

$$s(\tilde{G}_{n,r}) := \frac{9}{10} \min_{x \in \mathcal{C}_\sigma[X]} \left\{ \deg(x; \tilde{G}_{n,r}) \cdot \tilde{\pi}_{n,r}(x) \right\}, \quad \tilde{\Phi}_{n,r} = \min_{S \subseteq \mathcal{C}_\sigma[X]} \Phi(S; \tilde{G}_{n,r}). \quad (11)$$

190 We argue that the random walk over  $\tilde{G}_{n,r}$  quickly escapes sets with stationary distribution less  
 191 than  $s(\tilde{G}_{n,r})$ , and so we avoid a  $\log(1/\pi_0)$  ‘start penalty’ – where  $\pi_0 := \min_{x \in \mathcal{C}_\sigma[X]} \tilde{\pi}_{n,r} \lesssim \frac{1}{n}$  –  
 192 characteristic to analyses of mixing time, which would render any resultant upper bound on mixing  
 193 time vacuous. Instead, we obtain the tighter upper bound <sup>5</sup>

$$\tau_{n,r}(\mathcal{C}_\sigma[X]) \lesssim \frac{1}{\tilde{\Phi}_{n,r}^2} \log^2 \left( 1/s(\tilde{G}_{n,r}) \right).$$

194 Then,

- 195 • Some straightforward calculations yield  $s(\tilde{G}_{n,r}) \gtrsim \frac{\Lambda_\sigma r^d}{\lambda_\sigma}$ .
- 196 • To handle the conductance, we introduce a continuous analogue,

$$\tilde{\Phi}_{\mathbb{P},r} := \min_{\mathcal{S} \subseteq \mathcal{C}_\sigma} \left( \frac{\int_{\mathcal{S}} \mathbb{P}(B(x,r) \cap \mathcal{S}^c) f(x) dx}{\min \left\{ \int_{\mathcal{S}} \mathbb{P}(B(x,r) \cap \mathcal{C}_\sigma) f(x) dx, \int_{\mathcal{S}^c} \mathbb{P}(B(x,r) \cap \mathcal{C}_\sigma) f(x) dx \right\}} \right), \quad \mathcal{S}^c = \mathcal{C}_\sigma \setminus \mathcal{S} \quad (12)$$

197 and show the asymptotic lower bound  $\limsup_{n \rightarrow \infty} \tilde{\Phi}_{n,r} \gtrsim \tilde{\Phi}_{\mathbb{P},r}$ .

- 198 • Finally, we extend classical isoperimetric results lower bounding  $\tilde{\Phi}_{\mathbb{P},r}$ , when  $\mathbb{P}$  is uniform  
 199 and  $\mathcal{C}_\sigma$  convex, to hold under the more general conditions (A1) and (A4).

200 *Remark 3.* The embedding assumption (A4) and Lipschitz parameter  $L$  obviously play an important  
 201 role in the upper bound of Theorem 2. It is clear that there is some interdependence between  $L$   
 202 and other geometric parameters  $\sigma$  and  $D$ , which might lead one to hope that (A4) is non-essential.  
 203 However, it is not possible to eliminate this condition without incurring an additional factor of at  
 204 least  $(D/\sigma)^d$  in (10), achieved, for instance, when  $\mathcal{C}_\sigma$  consists of two balls of diameter  $D$  linked by  
 205 a cylinder of length  $D$  and radius  $\sigma$ . [Abbasi-Yadkori et al., 2017, Abbasi-Yadkori, 2016] develop  
 206 theory regarding biLipschitz deformations of convex sets, wherein it is observed that star-shaped sets  
 207 as well as half-moon shapes of the type we consider in Section 4 both satisfy (A4) for reasonably  
 208 small values of  $L$ .

## 209 3 Consistent Cluster Estimation

### 210 3.1 Well-Conditioned Density Clusters

211 For PPR to accurately estimate a set, the ratio of normalized cut to inverse mixing time should be  
 212 small. Letting  $\theta := (r, \sigma, \lambda, \lambda_\sigma, \Lambda_\sigma, \gamma, D, L)$  contain those parameters which govern the bounds  
 213 given in Theorems 1 and 2, further abbreviate

$$\Phi(\theta) := c_1 r \frac{d}{\sigma} \frac{\lambda}{\lambda_\sigma} \frac{(\lambda_\sigma - c_0 \frac{r^\gamma}{\gamma+1})}{\lambda_\sigma}$$

$$\Psi(\theta) := \left( c_2 \frac{\Lambda_\sigma^4 d^3 D^2 L^2}{\lambda_\sigma^4 r^2} \log^2 \left( \frac{1}{r} \right) + c_3 \log \left( \frac{\Lambda_\sigma}{\lambda_\sigma} \right) \right)^{-1}$$

214 for these bounds (where all constants  $c_0, c_1, c_2, c_3 > 0$  are as in these theorems).

215 Well-conditioned density clusters satisfy all of the given assumptions, for parameters which results in  
 216 ‘good’ values of  $\Phi(\theta)$  and  $\Psi(\theta)$ .

217 **Definition 3** (Well-conditioned density clusters). *For  $\lambda > 0$  and  $\mathcal{C} \in \mathbb{C}_f(\lambda)$ , let  $\mathcal{C}$  satisfy (A1) - (A4)  
 218 for some  $\sigma, \lambda, \lambda_\sigma, \Lambda_\sigma, \gamma, D, L > 0$ , and additionally let  $\mathcal{C}_\sigma$  satisfy (7). Then, setting*

$$\kappa(\mathcal{C}) := \frac{\Phi(\theta)}{\Psi(\theta)}$$

219 *we call  $\mathcal{C}$  a  $\kappa$ -well-conditioned density cluster (with respect to  $\theta$ ).*

<sup>5</sup>For sequences  $a_n, b_n$ , we write  $a_n \lesssim b_n$  ( $a_n \gtrsim b_n$ ) when there exists  $c > 0$  such that  $a_n \leq cb_n$  ( $a_n \geq cb_n$ ) for all sufficiently large  $n$ .

We focus for a moment on the neighborhood graph radius  $r$ . While taking  $r \rightarrow 0$  as  $n \rightarrow \infty$ —and thereby ensuring  $G_{n,r}$  is sparse—is computationally attractive, the presence of a factor of  $\frac{1}{r}$  in  $\kappa(\mathcal{C})$  unfortunately prevents us from making claims about the behavior of PPR in this regime. Although the restriction to a kernel function fixed in  $n$  is standard for theoretical analysis of spectral clustering Schiebinger et al. [2015], von Luxburg et al. [2008], it is an interesting question whether PPR exhibits some degeneracy over  $r$ -neighborhood graphs as  $r \rightarrow 0$ , or if this is merely looseness in our upper bounds.

**Well-conditioned clusters.** As is typical in the local clustering literature, our results will be stated with respect to specific choices or ranges of each of the user-specified parameters, which in this case may depend on the underlying (unknown) density.

In particular, for a well-conditioned density cluster  $\mathcal{C}$  (with respect to some  $\theta$ ), we require

$$r \leq \frac{\sigma}{2d}, \alpha \in [1/10, 1/9] \cdot \Psi(\theta),$$

$$v \in \mathcal{C}_\sigma[X]^g, \text{vol}_0 \in [3/4, 5/4] \cdot n(n-1) \int_{\mathcal{C}_\sigma} \mathbb{P}(B(x, r)) f(x) dx \quad (13)$$

where  $\mathcal{C}_\sigma[X]^g \subseteq \mathcal{C}_\sigma[X]$  is some ‘good’ subset of  $\mathcal{C}_\sigma[X]$  which, as we will see, satisfies  $\text{vol}(\mathcal{C}_\sigma[X]^g; G_{n,r}) \geq \text{vol}(\mathcal{C}_\sigma[X]; G_{n,r})/2$ . (Intuitively one can think of  $\mathcal{C}_\sigma[X]^g$  as consisting of the data sufficiently close to the center of  $\mathcal{C}_\sigma[X]$ , although we provide no formal justification to this effect.)

**Definition 4.** If the input parameters to Algorithm 1 satisfy (13) for some well-conditioned density cluster  $\mathcal{C}$ , we say the algorithm is well-initialized.

In practice, a reasonable way to choose these hyperparameters is by tuning. For example, if one wanted to successfully recover a density cluster, one could vary each hyperparameter over a grid, retaining outputs  $\hat{\mathcal{C}}$  of Algorithm 1 only if they recover some  $\mathcal{C} \in \mathbb{C}_f(\lambda)$  and discarding them otherwise. Then simply return the minimum normalized cut set from those  $\hat{\mathcal{C}}$  which were retained. Assuming there existed  $\lambda > 0, \mathcal{C} \in \mathbb{C}_f(\lambda)$  such that  $\mathcal{C}$  satisfied the conditions of Theorem 4, and moreover some combination of tuning parameters in the chosen grid satisfied (13), this scheme would inherit the consistency guarantees of Theorem 4.

**Misclassification error for PPR.** In Zhu et al. [2013], building on the work of Andersen et al. [2006] and others, theory is developed which links algorithmic performance of PPR to the normalized cut and mixing time parameters. This work, combined with the results of Section 2, immediately implies a bound on the volume of  $\hat{\mathcal{C}} \setminus \mathcal{C}_\sigma[X]$  (and likewise  $\mathcal{C}_\sigma[X] \setminus \hat{\mathcal{C}}$ ),

$$\text{vol}_{n,r}(\hat{\mathcal{C}} \setminus \mathcal{C}_\sigma[X]), \text{vol}_{n,r}(\mathcal{C}_\sigma[X] \setminus \hat{\mathcal{C}}) \lesssim \kappa(\mathcal{C}) \text{vol}_{n,r}(\mathcal{C}_\sigma[X]). \quad (14)$$

where we’ve written  $\text{vol}_{n,r}(S) := \text{vol}(S; G_{n,r})$  for  $S \subseteq X$ . To translate (14) into meaningful bounds on misclassification error, we wish to preclude vertices  $x \in X$  from having arbitrarily small degree. To do so, we make some regularity assumptions on  $\mathcal{X} = \text{supp}(f)$ .

(A5) *Valid region:*  $0 < \lambda_{\min} < f(x)$  for all  $x \in \mathcal{X}$ . Additionally, there exists some  $c > 0$  such that for each  $x \in \partial\mathcal{X}$ ,  $\nu(B(x, r) \cap \mathcal{X}) \geq c\nu(B(x, r))$ .

Note that the latter condition in (A5) will be satisfied if, for instance,  $\mathcal{X}$  is a  $\sigma$ -expansion.

**Theorem 3.** Fix  $\lambda > 0$ , let  $\mathcal{C} \in \mathbb{C}_f(\lambda)$  be a  $\kappa$ -well conditioned density cluster (with respect to some  $\theta$ ), and additionally assume  $f$  satisfies (A5). Then, with probability tending to one as  $n \rightarrow \infty$ ,

$$\frac{|\mathcal{C}_\sigma[X] \setminus \hat{\mathcal{C}}|}{|\mathcal{C}_\sigma[X]|} \leq c_5 \kappa(\mathcal{C}) \frac{\Lambda_\sigma}{\lambda_\sigma}, \quad \text{and} \quad \frac{|\hat{\mathcal{C}} \setminus \mathcal{C}_\sigma[X]|}{|\mathcal{C}_\sigma[X]|} \leq c_6 \kappa(\mathcal{C}) \frac{\Lambda_\sigma}{\lambda_{\min}}. \quad (15)$$

for universal constants  $c_4, c_5 > 0$ .

**Remark 4.** A notable implication of our theory is that as the diameter  $D$  increases, our upper bound on the normalized cut of  $\mathcal{C}_\sigma[X]$  remains unchanged, but  $\kappa(\mathcal{C})$ , and therefore the misclassification error, worsens (increases). This phenomenon reflects established wisdom regarding spectral partitioning



algorithms more generally Guattery and Miller [1995], Hein and Bühler [2010], albeit newly applied to the density clustering setting. It suggests that PPR may fail to recover  $\mathcal{C}_\sigma[X]$  even when  $\mathcal{C}$  is sufficiently well-conditioned to ensure  $\mathcal{C}_\sigma[X]$  has a small normalized cut in  $G_{n,r}$ . This intuition will be supported by simulations in Section 4.

**Consistent density cluster estimation.** Neither (14) nor Theorem 3 imply consistent density cluster estimation in the sense of (6). This notion of consistency requires a uniform bound over  $p$  for all  $u \in \mathcal{C}, u' \in \mathcal{C}'$

$$\frac{p_{u'}}{\mathbf{D}_{uu}} \leq \frac{1}{40\text{vol}_0} < \frac{1}{11\text{vol}_0} \leq \frac{p_u}{\mathbf{D}_{uu}}. \quad (16)$$

so that any sweep cut  $S_\beta$  for  $\beta\text{vol}_0 \in [1/40, 1/11]$  (i.e. any sweep cut considered by Algorithm 1) will fulfill both conditions laid out in (6). In Theorem 4, we show that a sufficiently small upper bound on  $\kappa(\mathcal{C})$  ensures such a gap exists with probability one as  $n \rightarrow \infty$ , and therefore guarantees  $\hat{\mathcal{C}}$  will be a consistent estimator.

As before, we wish to preclude arbitrarily low degree vertices, this time for points  $x \in \mathcal{C}'[X]$ .

(A6)  $\mathcal{C}'$ -bounded density : For each  $\mathcal{C}' \in \mathbb{C}_f(\lambda), \mathcal{C}' \neq \mathcal{C}$ , for all  $x \in \mathcal{C}' + \sigma B$ ,

$$\lambda_\sigma \leq f(x)$$

where  $\sigma, \lambda_\sigma$  are as in (A1).

**Theorem 4.** Fix  $\lambda > 0$ , let  $\mathcal{C} \in \mathbb{C}_f(\lambda)$  be a  $\kappa$ -well conditioned cluster (with respect to some  $\theta$ ), and additionally assume (A6) holds. If Algorithm 1 is well-initialized, there exists universal constant  $c_7 > 0$  such that if

$$\kappa(\mathcal{C}) \leq c_7 \frac{\lambda_\sigma^2 r^d \nu_d}{\Lambda_\sigma \mathbb{P}(\mathcal{C}_\sigma)}, \quad (17)$$

then the output set  $\hat{\mathcal{C}} \subseteq X$  is a consistent estimator for  $\mathcal{C}$ , in the sense of Definition 2.

**Cluster estimation with the approximate PPR vector.** As mentioned previously, in practice exactly solving (3) may be too computationally expensive. To address this limitation, Andersen et al. [2006] introduced the  $\epsilon$ -approximate PPR vector (aPPR), which we will denote  $p^{(\epsilon)}$ . We refer the curious reader to Andersen et al. [2006] for a formal algorithmic definition of the aPPR vector, and limit ourselves to highlighting a few salient points. Namely, the aPPR vector can be computed in  $\mathcal{O}(\frac{1}{\epsilon\alpha})$  time, while satisfying the following uniform error bound:

$$\text{for all } x \in X, \quad p(x) - \epsilon \deg_{n,r}(x) \leq p^{(\epsilon)}(x) \leq p(x) \quad (18)$$

Application of (18) within the proofs of Theorems 3 and 4 leads to analogous results which hold with respect to  $p^{(\epsilon)}$ .

**Corollary 1.** Fix  $\lambda > 0$ , and let  $\mathcal{C} \in \mathbb{C}_f(\lambda)$  be a  $\kappa$ -well-conditioned cluster (with respect to some  $\theta$ ). Choose input parameters  $\alpha, r, \text{vol}_0, v$  to be well-initialized in the sense of (13), set  $\epsilon = \frac{1}{20\text{vol}_0}$ , and modify Algorithm 1 to compute the aPPR vector  $p^{(\epsilon)}$  rather than the exact PPR vector  $p$ , with resulting output  $\hat{\mathcal{C}}$ .

1. Assume (A5) holds. Then (15) is still a valid upper bound for the misclassification error of  $\hat{\mathcal{C}}$ .

2. Assume (A6) holds. If

$$\kappa(\mathcal{C}) \leq c_7 \frac{\lambda_\sigma^2}{\Lambda_\sigma^2} \frac{r^d \nu_d}{\nu(\mathcal{C}_\sigma)}$$

then  $\hat{\mathcal{C}} \subseteq X$  is a consistent estimator for  $\mathcal{C}$ , in the sense of Definition 2.

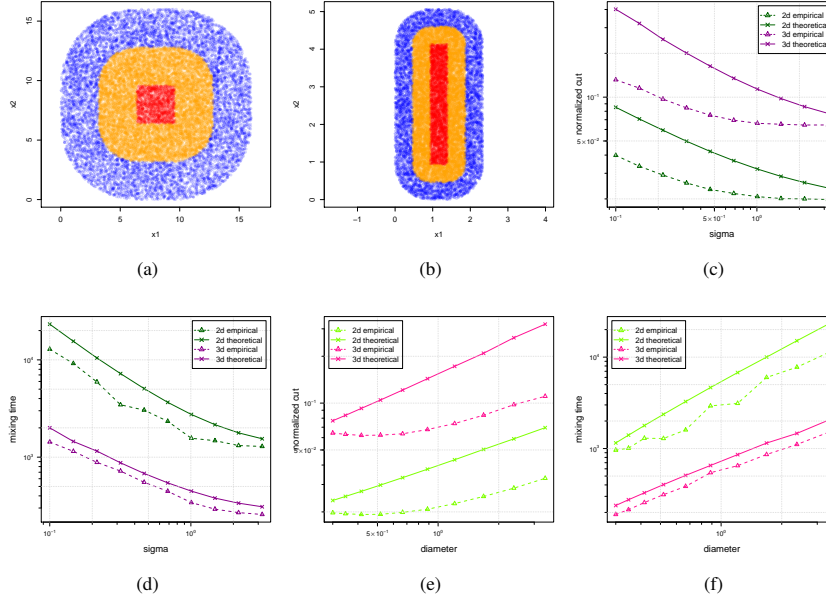


Figure 1: Samples, empirical results, and theoretical bounds for mixing time and normalized cut as diameter and thickness are varied. In (a) and (b), points in  $\mathcal{C}$  are colored in red; points in  $\mathcal{C}_\sigma \setminus \mathcal{C}$  are colored in yellow; and remaining points in blue.

## 294 4 Experiments

### 295 4.1 Validating Theoretical Bounds

296 As we do not provide any theoretical lower bounds, we validate the tightness of Theorems 1 and 2  
 297 via simulation. We sample points according to the density function  $q$ , where for  $x \in \mathbb{R}^d$

$$q(x) := \begin{cases} \lambda, & x \in [0, \sigma] \times D^{d-1} =: \mathcal{C}, \\ \lambda - \text{dist}(x, \mathcal{C})\eta, & x \in \mathcal{C}_\sigma \setminus \mathcal{C}, \\ (\lambda - \sigma\eta) - \text{dist}(x, \mathcal{C}_\sigma)^\gamma, & x \in (\mathcal{C}_\sigma + \sigma B) \setminus \mathcal{C}_\sigma, \\ 0, & \text{otherwise,} \end{cases} \quad (19)$$

298 where  $\lambda = \frac{150}{81}\sigma^\gamma$  and  $\eta = \frac{15}{81}\sigma^{\gamma-1}$ . Panels (a) and (b) in Figure 1 show 20,000 samples from  
 299 two parameterizations of  $q$ . In (a),  $\sigma = D = 3.2$ , while in (b)  $\sigma = .1$  and  $D = 3.2$ . (For both,  
 300  $d = 2$ ).

301 Panels (c) – (f) in Figure 1 show the change in normalized cut and mixing time, respectively, as the  
 302 parameters  $\sigma$  ((c) and (d)) and  $D$  ((e) and (f)) are varied. In panels (c) and (d)  $\sigma = .1 \cdot \sqrt{2}^j$ ,  $j =$   
 303  $1, \dots, 10$ , and  $D$  is fixed at 3.2. In panels (e) and (f),  $D = .1 \cdot \sqrt{2}^j$ ,  $j = 1, \dots, 10$  and  $\sigma$  is fixed  
 304 at .1. For each panel, the solid lines show, up to constants<sup>6</sup>, the theoretical upper bound, given by  
 305 Theorem 1 for panels (c) and (e) and Theorem 2 for panels (d) and (f). The dashed lines show the  
 306 computed empirical value, averaged over  $m$  trials ( $m = 100$  for the normalized cut, dashed lines in  
 307 panels (c) and (e), and  $m = 20$  for the mixing time, dashed lines in panel (d) and (f)). For each trial  
 308 across all parameters,  $r$ , the neighborhood graph radius, is set throughout to be as small as possible  
 309 such that the resulting graph is connected, for computational efficiency. Green lines correspond to  
 310 dimension  $d = 2$ , whereas purple/pink lines correspond to  $d = 3$ .

311 Panels (d) and (f) show the solid lines tracking closely to the dashed lines, in both 2 and 3 dimensions.  
 312 This provides empirical evidence that the upper bound on mixing time given by Theorem 2 has the  
 313 right dependency on both thickness parameter  $\sigma$  and diameter  $D$ .

<sup>6</sup>Note that we have rescaled all values of theoretical upper bounds by a constant, in order to mask the effect of large universal constants in these bounds. Therefore only comparison of slopes, rather than intercepts, is meaningful.

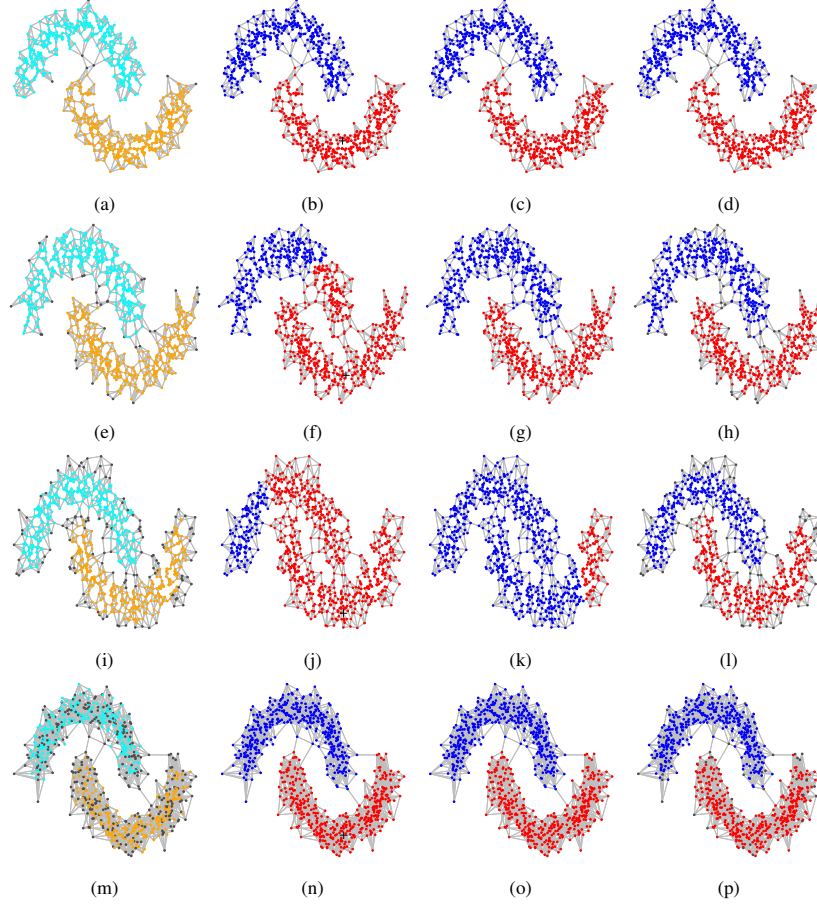


Figure 2: True density (column 1), PPR (column 2), normalized cut (column 3) and estimated density (column 4) clusters for 4 different simulated data sets. Seed node for PPR denoted by a black cross.

314 The story in panels (c) and (e) is less obvious. We note that while, broadly speaking, the trends do  
 315 not appear to match, this gap between theory and empirical results seems largest when  $\sigma \approx D$ ; this  
 316 is the right hand side on panel (c) and the left hand side on panel (e). It is in these regions that the  
 317 slopes of the dashed and solid lines are most different. As the ratio  $D/\sigma$  grows, we see the slopes of  
 318 the empirical curves becoming more similar to those predicted by theory. The takeaway message is  
 319 that while the dependency in (9) on  $\sigma$  and  $D$  is loose for clusters with diameter close to thickness, it  
 320 becomes tighter as  $D/\sigma$  grows.

## 321 4.2 Empirical PPR, normalized cut, and density clustering comparison

322 To drive home the main implications of Theorems 3 and 4, we show the behavior of PPR, normalized  
 323 cut, and the density clustering algorithm of [Chaudhuri and Dasgupta, 2010] on (a variant of) the  
 324 famous 'two moons' dataset, considered a prototypical success story for spectral clustering algorithms.  
 325 To form each of the four rows in Figure 2, 800 points are independently sampled following a 'two  
 326 moons plus Gaussian noise model'. Formally, the (respective) generative models for the data  
 327 are

$$Z \sim \text{Bern}(1/2), \theta \sim \text{Unif}(0, \pi) \quad (20)$$

$$X(Z, \theta) = \begin{cases} \mu_1 + (r \cos(\theta), r \sin(\theta)) + \sigma \epsilon, & \text{if } Z = 1 \\ \mu_2 + (r \cos(\theta), -r \sin(\theta)) + \sigma \epsilon, & \text{if } Z = 0 \end{cases} \quad (21)$$

328 where

$$\mu_1 = (-.5, 0), \mu_2 = (0, 0), \epsilon \sim N(0, I_2) \quad (\text{row 1})$$

$$\mu_1 = (-.5, -.07), \mu_2 = (0, .07), \epsilon \sim N(0, I_2) \quad (\text{row 2})$$

$$\mu_1 = (-.5, -.125), \mu_2 = (0, .125), \epsilon \sim N(0, I_2) \quad (\text{row 3})$$

$$\mu_1 = (-.5, -.025), \mu_2 = (0, .025), \epsilon \sim N(0, I_{10}) \quad (\text{row 4})$$

329 for  $I_d$  the  $d \times d$  identity matrix. The first column consists of the empirical density clusters  $C_n$  and  
 330  $C'_n$  for a particular threshold  $\lambda$  of the density function; the second column shows the PPR plus  
 331 minimum normalized sweep cut cluster, with hyperparameter  $\alpha$  and all sweep cuts considered; the  
 332 third column shows the global minimum normalized cut, computed according to the algorithm of  
 333 Szlam and Bresson [2010]; and the last column shows a cut of the density cluster tree estimator of  
 334 Chaudhuri and Dasgupta [2010].

335 Rows 1-3 show the degrading ability of PPR to recover density clusters as the two moons become less  
 336 salient. In the first row, the normalized cut conforms to the density cluster, and PPR recovers both.  
 337 In the second row, the normalized cut still conforms to the density cluster, but because the internal  
 338 connectivity of the lower moon is low, PPR fails to recover the normalized cut. In the third row, the  
 339 moons have such low saliency that even the normalized cut fails to recover the lower moon; we also  
 340 see from  $(k)$  that PPR does not somehow save us in this situation. Note that this is not a function  
 341 of the finite sample: the 4th column shows us that a well-designed density clustering algorithm can  
 342 recover the true density cluster.

343 The fourth row illustrates the effect of dimension. The gray dots in  $(m)$  (as in  $(a)$ ,  $(e)$  and  $(i)$  are  
 344 observations in low-density regions. While the PPR sweep cut  $(n)$  has relatively high symmetric set  
 345 difference with the chosen density cut, it still recovers  $C_n$  in the sense of Definition 2.

## 346 5 Discussion

347 For a clustering algorithm and a given object (such as a graph or set of points), there are an almost  
 348 limitless number of ways to define what the 'right' clustering is. We have considered a few such ways  
 349 – density level sets, and the bicriteria of normalized cut, inverse mixing time – and shown that under  
 350 the right conditions, the latter agree with the former, with resulting algorithmic consequences.

351 We do not provide a theoretical lower bound showing that our geometric conditions are required for  
 352 successful recovery on an upper level set. Although we investigate the matter empirically, this is a  
 353 direction for future work.

## References

- Yasin Abbasi-Yadkori. Fast mixing random walks and regularity of incompressible vector fields. *arXiv preprint arXiv:1611.09252*, 2016.
- Yasin Abbasi-Yadkori, Peter Bartlett, Victor Gabillon, and Alan Malek. Hit-and-Run for Sampling and Planning in Non-Convex Spaces. In *Proceedings of the 20th International Conference on Artificial Intelligence and Statistics*, pages 888–895, 2017.
- Emmanuel Abbe. Community detection and stochastic block models. *Foundations and Trends® in Communications and Information Theory*, 14(1-2):1–162, 2018.
- Reid Andersen and Yuval Peres. Finding sparse cuts locally using evolving sets. In *Proceedings of the Forty-first Annual ACM Symposium on Theory of Computing*, STOC '09, pages 235–244, New York, NY, USA, 2009. ACM. ISBN 978-1-60558-506-2. doi: 10.1145/1536414.1536449.
- Reid Andersen, Fan Chung, and Kevin Lang. Local graph partitioning using pagerank vectors. In *Proceedings of the 47th Annual IEEE Symposium on Foundations of Computer Science*, pages 475–486, 2006.
- Reid Andersen, David F Gleich, and Vahab Mirrokni. Overlapping clusters for distributed computation. In *Proceedings of the fifth ACM international conference on Web search and data mining*, pages 273–282. ACM, 2012.
- Sivaraman Balakrishnan, Min Xu, Akshay Krishnamurthy, and Aarti Singh. Noise thresholds for spectral clustering. In *Advances in Neural Information Processing Systems 24*. Curran Associates, Inc., 2011.
- Kamalika Chaudhuri and Sanjoy Dasgupta. Rates of convergence for the cluster tree. In J. D. Lafferty, C. K. I. Williams, J. Shawe-Taylor, R. S. Zemel, and A. Culotta, editors, *Advances in Neural Information Processing Systems 23*, pages 343–351. Curran Associates, Inc., 2010.
- Kamalika Chaudhuri, Fan Chung Graham, and Alexander Tsiatas. Spectral clustering of graphs with general degrees in the extended planted partition model. In *COLT*, volume 23, pages 35.1–35.23, 2012.
- W. E. Donath and A. J. Hoffman. Lower bounds for the partitioning of graphs. *IBM J. Res. Dev.*, 17(5):420–425, September 1973.
- Miroslav Fiedler. Algebraic connectivity of graphs. *Czechoslovak Mathematical Journal*, 23(2): 298–305, 1973.
- Santo Fortunato. Community detection in graphs. *Physics Reports*, 486(3):75–174, 2010.
- Shayan Oveis Gharan and Luca Trevisan. Approximating the expansion profile and almost optimal local graph clustering. In *Foundations of Computer Science (FOCS), 2012 IEEE 53rd Annual Symposium on*, pages 187–196. IEEE, 2012.
- David F Gleich and C Seshadhri. Vertex neighborhoods, low conductance cuts, and good seeds for local community methods. In *Proceedings of the 18th ACM SIGKDD international conference on Knowledge discovery and data mining*, pages 597–605. ACM, 2012.
- Stephen Guattery and Gary L Miller. On the performance of spectral graph partitioning methods. In *SODA*, volume 95, pages 233–242, 1995.
- John A. Hartigan. Consistency of single-linkage for high-density clusters. *Journal of the American Statistical Association*, 1981.
- Taher H Haveliwalla. Topic-sensitive pagerank: A context-sensitive ranking algorithm for web search. *IEEE transactions on knowledge and data engineering*, 15(4):784–796, 2003.
- Matthias Hein and Thomas Bühler. An inverse power method for nonlinear eigenproblems with applications in 1-spectral clustering and sparse pca. In *Advances in Neural Information Processing Systems*, pages 847–855, 2010.

400 Matthias Hein, Jean-Yves Audibert, and Ulrike von Luxburg. From graphs to manifolds – weak and  
401 strong pointwise consistency of graph laplacians. In *Learning Theory*, 2005.

402 Ravi Kannan, Santosh Vempala, and Adrian Vetta. On clusterings: Good, bad and spectral. *J. ACM*,  
403 51(3):497–515, May 2004.

404 Vladimir Koltchinskii and Evarist Giné. Random matrix approximation of spectra of integral operators.  
405 *Bernoulli*, 6(1):113–167, 02 2000.

406 Jing Lei and Alessandro Rinaldo. Consistency of spectral clustering in stochastic block models. *Ann.*  
407 *Statist.*, 43(1):215–237, 02 2015.

408 Jure Leskovec, Kevin J. Lang, and Michael Mahoney. Empirical comparison of algorithms for  
409 network community detection. In *Proceedings of the 19th International Conference on World Wide*  
410 *Web*, 2010.

411 Michael W. Mahoney, Lorenzo Orecchia, and Nisheeth K. Vishnoi. A local spectral method for  
412 graphs: with applications to improving graph partitions and exploring data graphs locally. *Journal*  
413 *of Machine Learning Research*, 13:2339–2365, 2012.

414 Frank McSherry. Spectral partitioning of random graphs. In *FOCS*, pages 529–537, 2001.

415 Karl Rohe, Sourav Chatterjee, and Bin Yu. Spectral clustering and the high-dimensional stochastic  
416 blockmodel. *Ann. Statist.*, 39(4):1878–1915, 08 2011.

417 Geoffrey Schiebinger, Martin J. Wainwright, and Bin Yu. The geometry of kernelized spectral  
418 clustering. *Ann. Statist.*, 43(2):819–846, 04 2015.

419 Tao Shi, Mikhail Belkin, and Bin Yu. Data spectroscopy: Eigenspaces of convolution operators and  
420 clustering. *Ann. Statist.*, 37(6B):3960–3984, 12 2009.

421 Aarti Singh, Clayton Scott, and Robert Nowak. Adaptive hausdorff estimation of density level sets.  
422 *Ann. Statist.*, 37(5B):2760–2782, 10 2009.

423 Daniel A Spielman and Shang-Hua Teng. Spectral sparsification of graphs. *SIAM Journal on*  
424 *Computing*, 40(4):981–1025, 2011.

425 Daniel A Spielman and Shang-Hua Teng. A local clustering algorithm for massive graphs and its  
426 application to nearly linear time graph partitioning. *SIAM Journal on Computing*, 42(1):1–26,  
427 2013.

428 Daniel A Spielman and Shang-Hua Teng. Nearly linear time algorithms for preconditioning and  
429 solving symmetric, diagonally dominant linear systems. *SIAM Journal on Matrix Analysis and*  
430 *Applications*, 35(3):835–885, 2014.

431 Arthur Szlam and Xavier Bresson. Total variation, cheeger cuts. In *ICML*, pages 1039–1046, 2010.

432 David Tolliver and Gary L. Miller. Graph partitioning by spectral rounding: Applications in image  
433 segmentation and clustering. In *Computer Vision and Pattern Recognition, CVPR*, volume 1, pages  
434 1053–1060, 2006.

435 Santosh Vempala and Grant Wang. A spectral algorithm for learning mixture models. *Journal of*  
436 *Computer and System Sciences*, 68(4):841 – 860, 2004.

437 Ulrike von Luxburg. A tutorial on spectral clustering. *Statistics and Computing*, 17(4):395–416,  
438 December 2007.

439 Ulrike von Luxburg, Mikhail Belkin, and Olivier Bousquet. Consistency of spectral clustering. *Ann.*  
440 *Statist.*, 36(2):555–586, 04 2008.

441 Xiao-Ming Wu, Zhenguo Li, Anthony M. So, John Wright, and Shih fu Chang. Learning with partially  
442 absorbing random walks. In F. Pereira, C. J. C. Burges, L. Bottou, and K. Q. Weinberger, editors,  
443 *Advances in Neural Information Processing Systems 25*, pages 3077–3085. Curran Associates, Inc.,  
444 2012.

- 445 Jaewon Yang and Jure Leskovec. Defining and evaluating network communities based on ground-truth.  
446 *Knowledge and Information Systems*, 42(1):181–213, Jan 2015.
- 447 Zeyuan Allen Zhu, Silvio Lattanzi, and Vahab S Mirrokni. A local algorithm for finding well-  
448 connected clusters. In *ICML (3)*, pages 396–404, 2013.